

## Incompressible flow over a NACA 0012 airfoil profile

Mohamed Fadol Orsod Ornasir  
*IIT Bombay*

### Synopsis

This research migration project aims to do numerical simulations of the flow over a NACA 0012 airfoil profile using OpenFOAM Version v2012. The geometry and mesh were defined using blockMesh utility. A steady-state, SIMPLE algorithm-based simpleFoam solver was used to simulate the problem. For accurate turbulence predictions, Spalart–Allmaras model were used and compared with the experimental data. Numerical calculations of the 2-D flow over the airfoil are presented, and results are compared against the results of two-dimensional wind tunnel tests of the symmetrical NACA 0012 airfoil reported in reference [1].

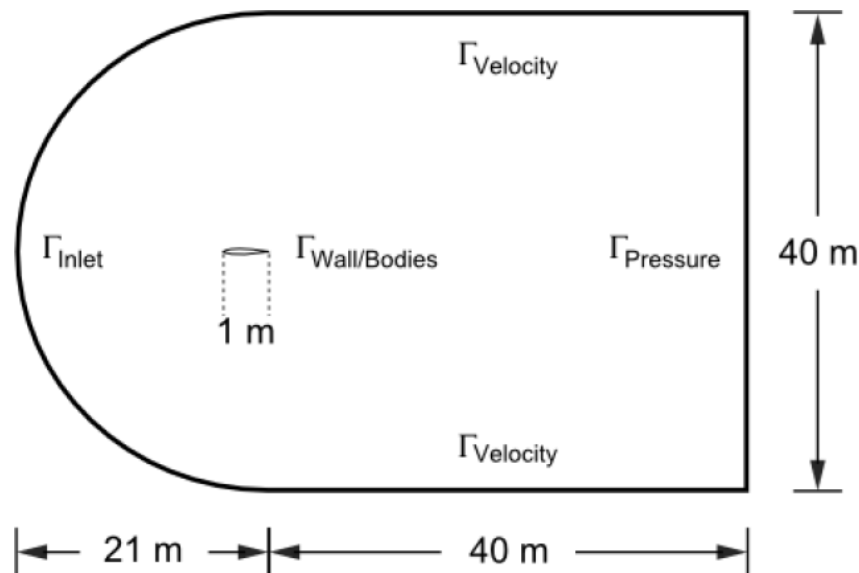


Figure (1): Geometry, Dimensions and Boundary condition

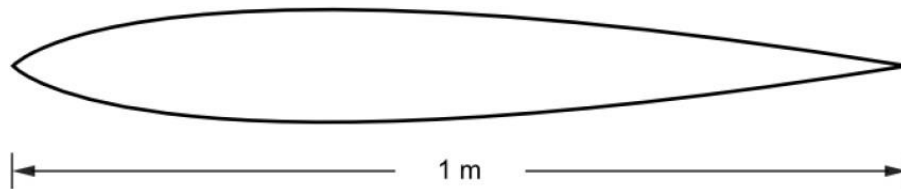
The dimensions of the geometry shown in the figure 1. The flow velocity is taken as 10m/s, resulting in a Mach number well below 0.3, and therefore the fluid model is assumed to be incompressible. Flowing fluid is entering from inlet with velocity of 10 m/s and exiting from outlet. Fluid properties and boundary conditions are discussed in the report.

### Reference

1. Two-dimensional aerodynamic characteristics of the NACA 0012 airfoil in the Langley 8-foot transonic pressure tunnel. NASA Technical Memorandum 81927. 1981.

## 1 Introduction

This case studies the flow over a NACA 0012 airfoil profile. Numerical calculations of the 2-D flow over the airfoil are presented, and results are compared against the reference paper results of two-dimensional wind tunnel tests of the symmetrical NACA 0012 airfoil reported in reference [1]. The incompressible flow over the airfoil is performed in a 2D analysis domain  $W$ . Several configurations have been studied by varying the angle of attack,  $\alpha$  ( $a$ ), in the range  $0 < a < 12$ . In addition, pressure distribution over the airfoil, is evaluated. Lift coefficient as a function of the angle of attack had calculated. Solutions are obtained for  $Re = 3.0 \cdot 10^6$ . The flow velocity is taken as 10m/s, resulting in a Mach number well below 0.3, and therefore, the fluid model is assumed to be incompressible. Detailed experimental results concerning the Mach number can also be found in reference [1]. Spallart-Allmaras turbulence model was initialized by using a value of the turbulent kinetic energy  $K_t = 0.00135 \text{ m}^2/\text{s}^2$  and a characteristic turbulent length  $L_t = 0.01 \text{ m}$ . A two-dimensional geometry is considered in the reference paper from data given in the test cases.



NACA 0012 airfoil profile. Chord length is 1.0 m.

## 2 Governing Equations and Models

To reproduce results generated in reference paper [1], OpenFOAM 2012v software was used. The Navier-Stokes equations for single-phase flows govern the simulation and are later compiled with 2-equation based turbulence models to capture turbulence in the flow. The governing continuity and momentum equations are given by:

### 2.1 Governing Equations

Continuity equation:

$$\nabla \cdot u = 0$$

Momentum equation:

$$\nabla \cdot (u \otimes u) - \nabla \cdot R = -\nabla p + S_u$$

### 2.2 Turbulence Model

Several turbulence models are available in the OpenFOAM 2012v. The Spallart-Allmaras turbulence models (2-eqn. based) employed in this research migration project and compared.

### 2.2.1 Spalart-Allmaras turbulence models:

The Spalart and Allmaras (1992) model is a one-equation model for kinematic eddy (turbulent) viscosity that solves a modelled transport equation. It was created primarily for aerospace applications involving wall-bounded flows, and it has consistently produced good results for boundary layers subjected to a wide range of pressure gradients. It's also becoming more common in turbomachinery applications. It is effectively a low Reynolds number model in its original form, requiring sufficient resolution of the viscous-affected portion of the boundary layer. The model's near-wall gradients of the transported variable are substantially smaller than the  $k - \epsilon$  or  $k - \omega$  models' gradients. [2]

The Spalart-Allmaras turbulence model is a one-equation turbulence model designed for aerodynamic flows. This model is an eddy viscosity transport equation. [3].

$$\frac{DF}{DT} = \frac{\partial F}{\partial t} + (u \cdot \nabla)F = \text{diffusion} + \text{production} - \text{destruction}$$

To build a complete model for a turbulent flow, each of the diffusion, production, and destruction variables must be precisely described. When these terms are defined and made non-dimensional, they get certain extra constants and non-dimensional functions. The transport equation for the working variable  $\tilde{\nu}$  is given by:

$$\begin{aligned} \frac{D\tilde{\nu}}{Dt} &= c_{b1}(1-f_{t2})\tilde{S}\tilde{\nu} + \frac{1}{\sigma}[\nabla \cdot ((\mathbf{v} + \tilde{\mathbf{v}}))\nabla\tilde{\nu} + c_{b2}(\nabla\tilde{\nu})^2] - \left(c_{w1}f_w - \frac{c_{b1}}{\kappa^2}f_{t2}\right)\left(\frac{\tilde{\nu}}{d}\right)^2 + f_{t1}\Delta U^2 \\ \tilde{S} &\equiv S + \frac{\tilde{\nu}}{\kappa^2 d^2} \left[ 1 - (\tilde{\nu}/\nu) \left[ 1 + \frac{(\tilde{\nu}/\nu)^4}{[(\tilde{\nu}/\nu)^3 + C_{v1}^3]} \right]^{-1} \right] \\ f_w &= \frac{\tilde{\nu}}{\tilde{S}\kappa^2 d^2} \left[ 1 + C_{w2} \left( \left( \frac{\tilde{\nu}}{\tilde{S}\kappa^2 d^2} \right)^5 - 1 \right) \right] (1 + C_{w3}^6)^{1/6} \left\{ \left[ 1 + C_{w2} \left( \left( \frac{\tilde{\nu}}{\tilde{S}\kappa^2 d^2} \right)^5 - 1 \right) \right]^6 + C_{w3}^6 \right\}^{-1/6} \\ f_{t1} &= C_{t1} g_t \exp \left[ -C_{t2} \frac{\omega_t^2}{\Delta U^2} (d^2 + g_t^2 d_t^2) \right], \quad f_{t2} = C_{t3} \exp \left[ -C_{t4} (\tilde{\nu}/\nu)^2 \right] \end{aligned}$$

where  $S$  is the magnitude of the vorticity,  $d$  is the distance to the closest wall,  $dt$  is the distance from the point in the flow field to the trip on the wall,  $\omega_t$  is the wall vorticity at the trip,  $\Delta U$  is the difference between velocity at the field point and that at the trip,  $g_t = \min(0.1, \Delta U/Wt \Delta x_t)$  where  $\Delta x_t$  is the grid spacing along the wall at the trip. The empirical constants of the Spalart-Allmaras model are:  $C_{b1} = 0.1355$ ,  $\sigma = 2/3$ ,  $C_{b2} = 0.622$ ,  $\kappa = 0.4187$ ,  $C_{w1} = 3.239$ ,  $C_{w2} = 0.3$ ,  $C_{w3} = 2.0$ ,  $C_{v1} = 7.1$ ,  $C_{t1} = 1$ ,  $C_{t2} = 2$ ,  $C_{t3} = 1.2$  and  $C_{t4} = 0.5$  [3].

## 3 Simulation Procedure

### 3.1 Geometry and Mesh

In this work, blockMesh is used to create a 2D mesh for a NACA 0012 airfoil. As indicated in the diagram below, the mesh is separated into four blocks. MergePatch, Spline, and complicated edgeGrading are among the approaches used to reduce the number of blocks as much as feasible. Spline approximates the complex form of the airfoil. The coordinates of points 1 and 16, as well as 5 and 17, are the same. Blocks 2 and 4 do not share any faces, however, because they are specified as independent points. As a result, mergePatch is required to join these two blocks. Complex edgeGrading ensures the boundary layer on the airfoil, eliminating the need to divide the boundary layer into a distinct block.

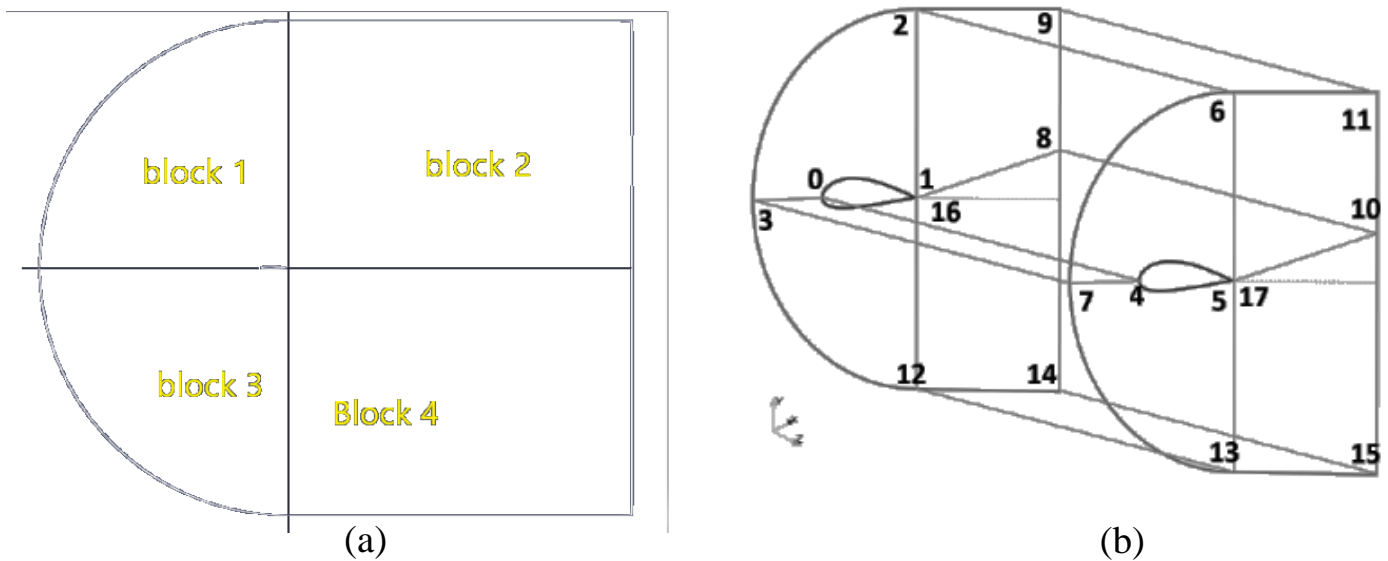
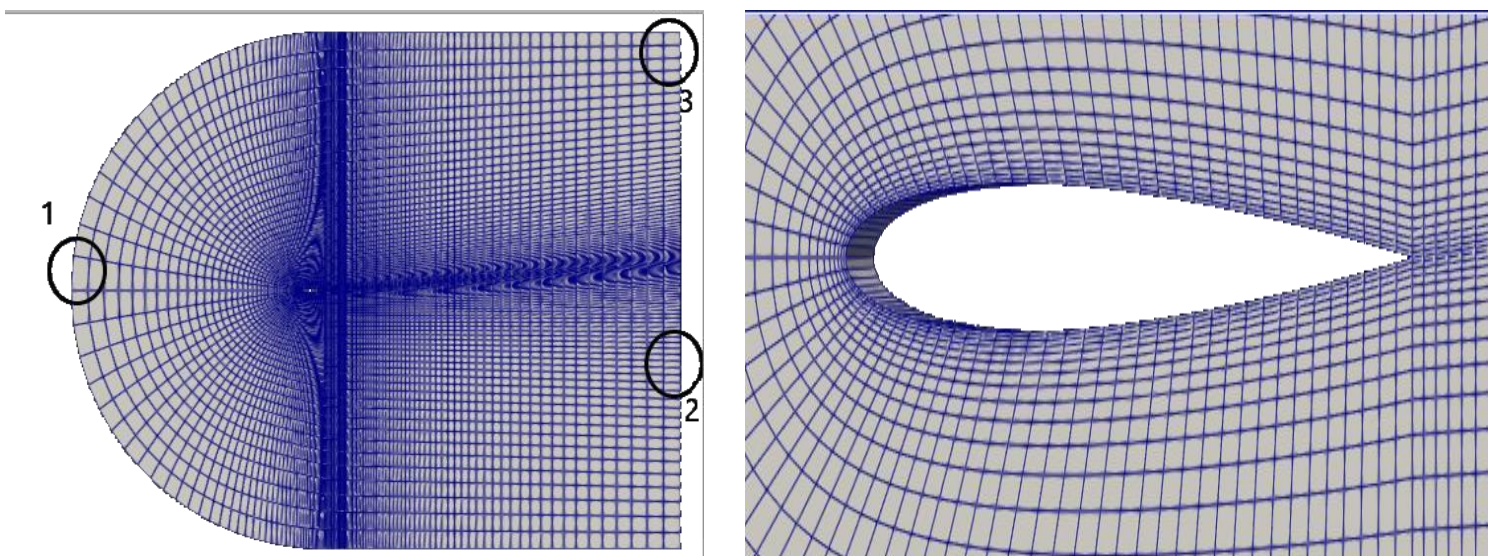


Figure (2): vertices and blocks

The Input Parameter for mesh at far field: Max cell size in inlet =1, max cell size in outlet =1 and max cell size in inlet x outlet=1, show figure (3,a). Meshing Airfoil Boundary: Cell size at leading edge =0.01 Cell size at trailing edge =0.03 Cell size at middle = 0.035 see figure (3,b)



(a)

(b)

Figure 3 mesh parameter

The Input parameter for Boundary layer: Boundary layer thickness=0.5, first layer thickness =0.005, expansion Ratio= 1.2, see figure (3,b). The final geometry and mesh shown in figure (4).

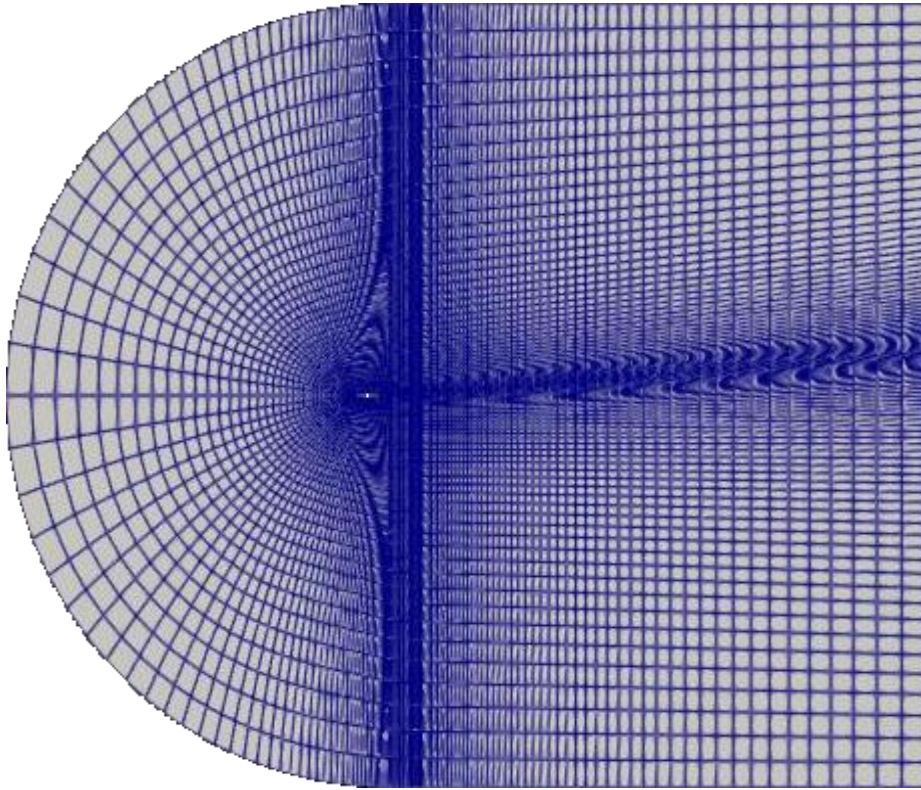


Figure (4) Final geometry

### 3.2 Initial and Boundary Conditions

An inlet, outlet, top, bottom and wall are the five boundaries that need boundary conditions. Front and back are the other two boundaries, both of which are empty.

Inlet: fix velocity condition is specified at the left side of the control volume which has been discretized by using a C-grid. Outlet: fix pressure is specified at the right side of the control volume. Wall: V Fix Wall condition has been used in order to enforce the no-slip condition at the surface of the airfoil. Other: null normal velocity (free-slip) has been enforced at the top and bottom edges of the control volume.

Initial conditions, Velocity was initialized within the entire domain to the value specified at the inlet boundary 10 m/s. Pressure, automatically initialized to 0.0. Turbulence model: the Spallart-Allmaras turbulence model was initialized by using a value of the turbulent kinetic energy  $K_t = 0.00135 \text{ m}^2/\text{s}^2$  and a characteristic turbulent length  $L_t = 0.01 \text{ m}$ . No particular adjustment of the turbulence model was undertaken in the present analysis.

Table 1: Boundary condition

	Initial	inlet	outlet	walls
$U [m^2s^{-1}]$	0	10	ZG	noSlip
$p [m^2s^{-2}]$	0	ZG	0	ZG

### 3.3 Solver

To solve governing equations in the discretized domain, the steady-state for incompressible, turbulent flow-based simpleFoam solver is employed. The SIMPLE (Semi-Implicit Method for Pressure Linked Equations) technique is used by the simpleFoam solver to analyse NS equations. A segregated solution technique is used by the solver. This implies that the equations for each variable that characterises the system (velocity  $u$ , pressure  $p$ , and turbulence variables) are solved sequentially. In the next equation, the solutions to the previous equations are entered. For the convergence, conditional strategy used with 2000 maximum iterations or  $10^5$  convergences criteria. The Spallart-Allmaras turbulence model cases at zero angle of attack converged at 1191 and 1226 iterations, respectively.

## 4 Grid independence study and validation:

### 4.1 Grid independence Test:

Airfor had simulated with a zero angle of attack. For test1, test 2, and test 3, the number of cells is modified to 11040, 42000, and 132000, respectively, we can observe that there is no change in maximum velocity when change mesh.

### 4.2 Validation:

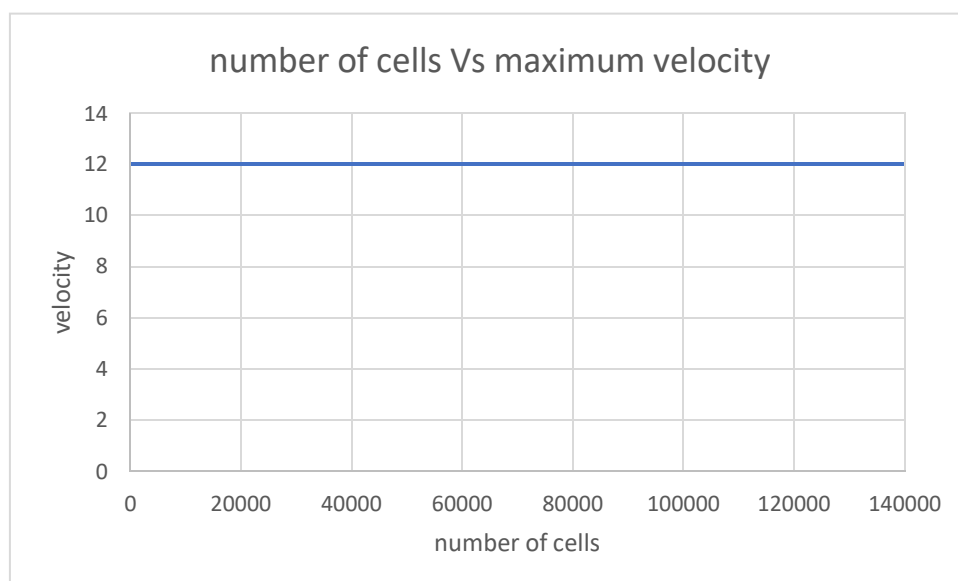


Figure (5) Grid independent test

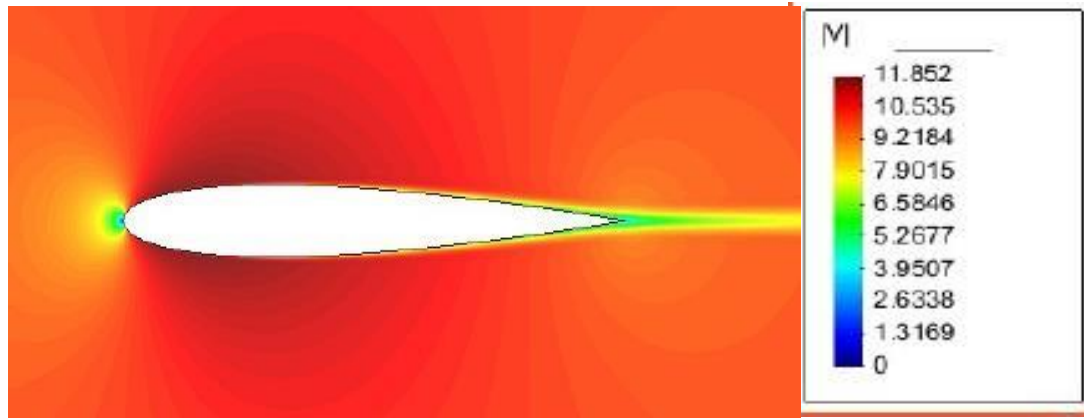


Figure (6) validation

From figure (5) and figure (6), we can observe that openFoam vs reference paper has approximately same maximum velocity with 1.2% error.

## 5 Results and Discussions

For the comparison of the results, velocity contour, pressure contour lift coefficient with different angle of attack taken place. The results were compared with the experimental data or the reference paper. [1]. Figure (7), figure (8), figure (9) and figure (10) shown the velocity contour, pressure contour, lift coefficient and pressure coefficient with different angle of attack, respectively.

The figures below (8) and (9) show the velocity contour and pressure contour for the given mesh and for zero angles of attack. The results compared against results reported in reference [1].

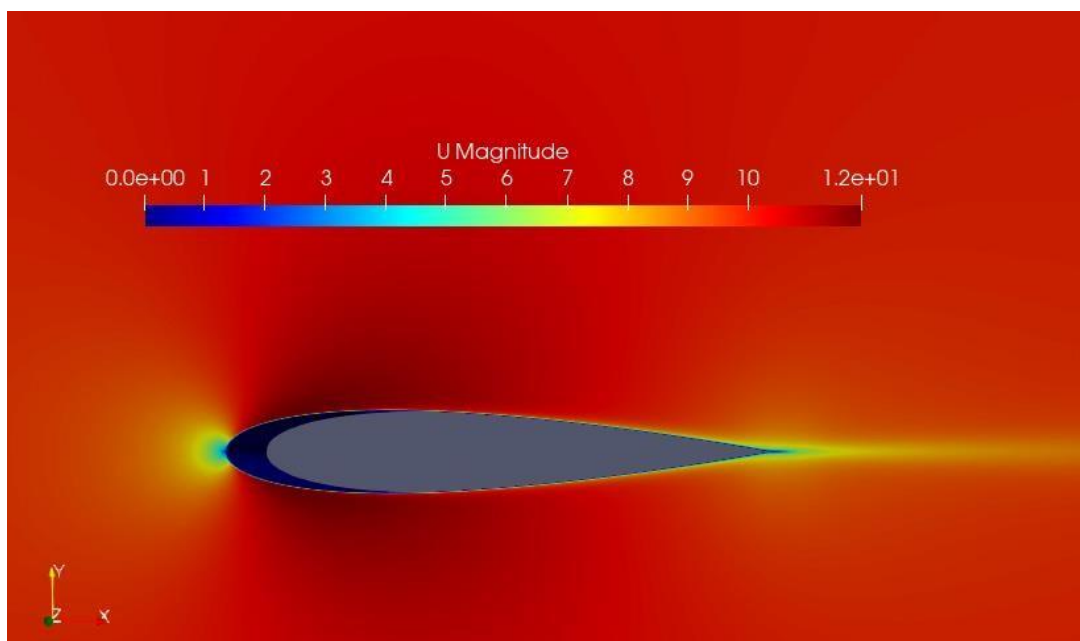


Figure (7) velocity field at 0 angle of attack

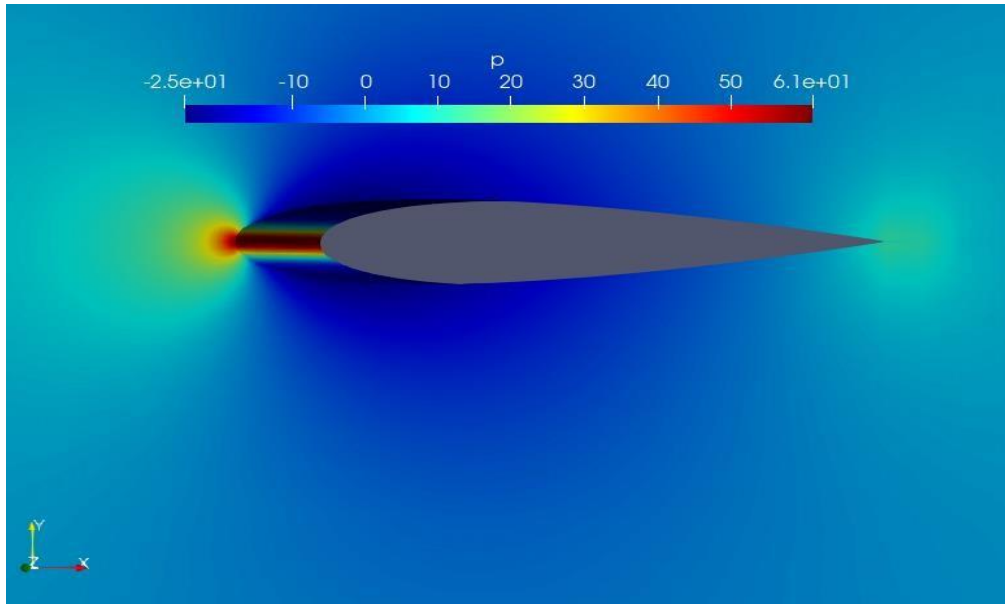


Figure (8) Pressure field at 0 angle of attack

Reference results:

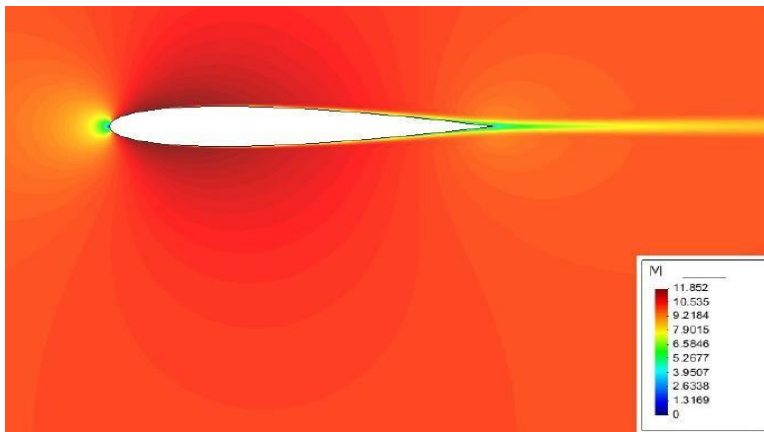


Figure (8, a) Velocity contour 0deg

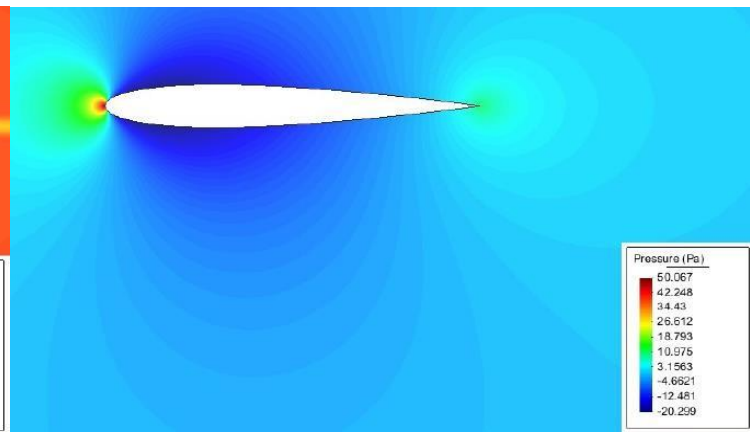


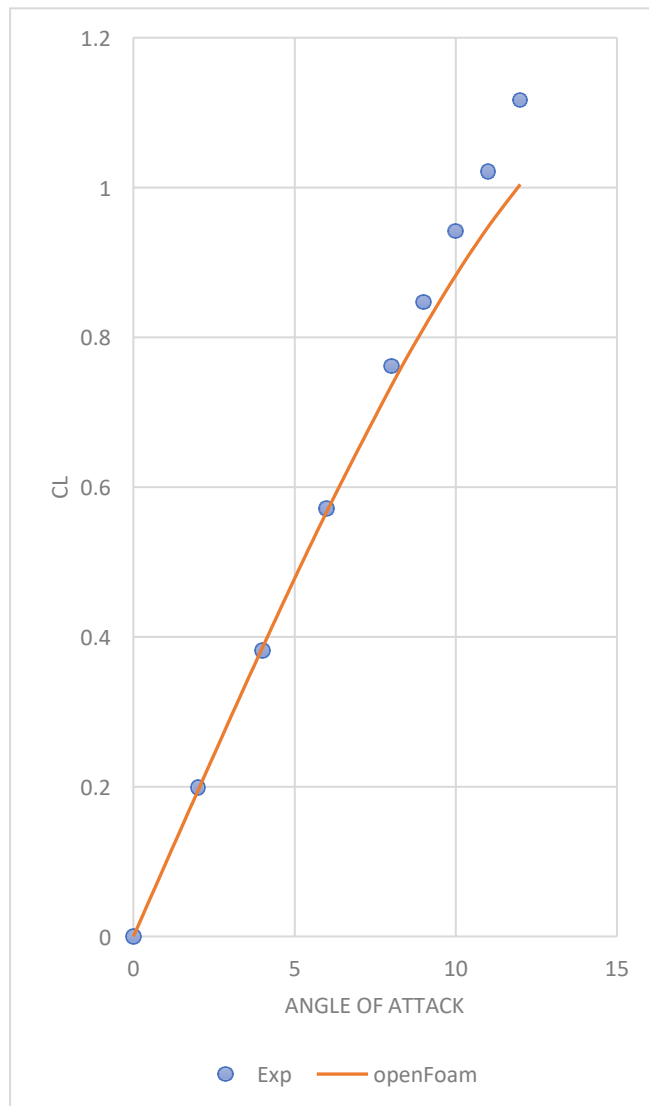
Figure (8, b) pressure contour 0deg

Fig (9) shows the lift coefficient as a function of the angle of attack. Simulation results (solid lines) are compared against experimental results (solid dots) reported in reference [1].

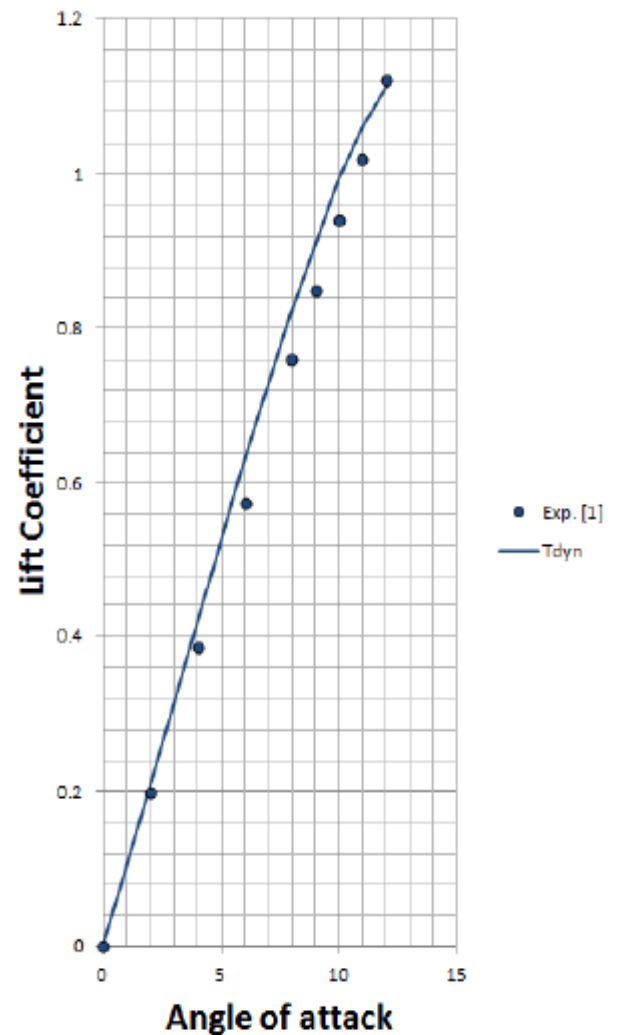
**Table (2) compare value of lift coefficient with experimental data:**

Angle of attack	Lift coefficient (OpenFoam)	Lift Coefficient ( experimentally)
0	0.00000419	0
2	0.1945114	0.19887
4	0.385488	0.381921
6	0.567346	0.571751
8	0.734898	0.761582
9	0.811642	0.847458
10	0.882756	0.942373
11	0.94714	1.021469
12	1.004134	1.116384

In the range below the critical angle of attack  $0 < \alpha < 12^\circ$ , OpenFoam findings are in good agreement with the lift values obtained in the experiments.



OpenFoam results



reference result

Figure (9) lift coefficient as a function of the angle of attack

The pressure coefficient distributions along the normalised airfoil profile at 1.86 angles of attack are shown in the figures below figure (5). Simulation results compared to the experimental results reported in reference [1]. Usually, not the pressure but the ratio of the local pressure to the stagnation pressure is plotted, known as pressure Coefficient ( $C_p$ ), follows,

$$C_p = \frac{P - P_{inf}}{0.5 \times \rho \times v^2}$$

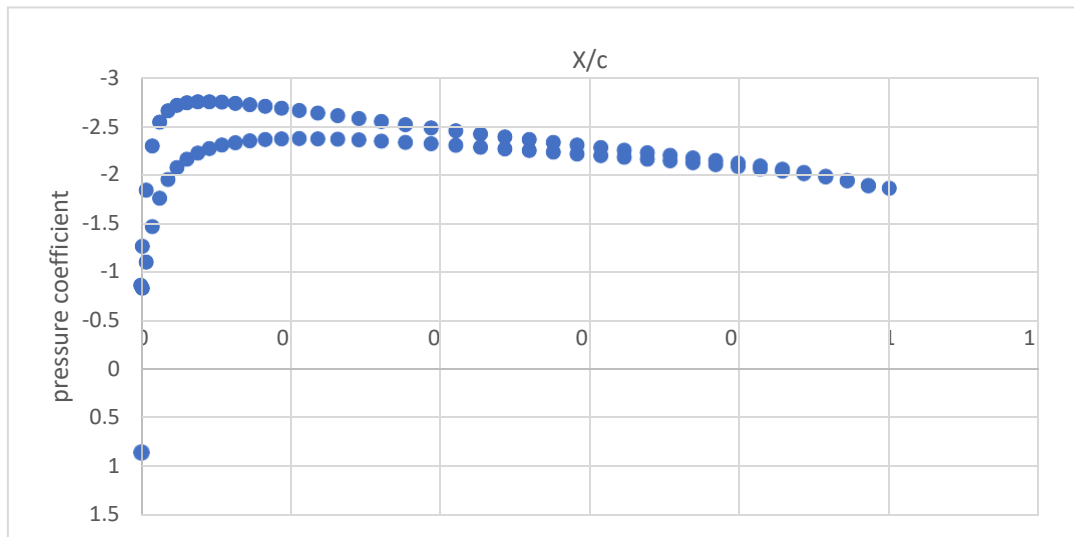


Figure (10) pressure coefficient with x axis at 1.86 angle of attack

Results from reference:

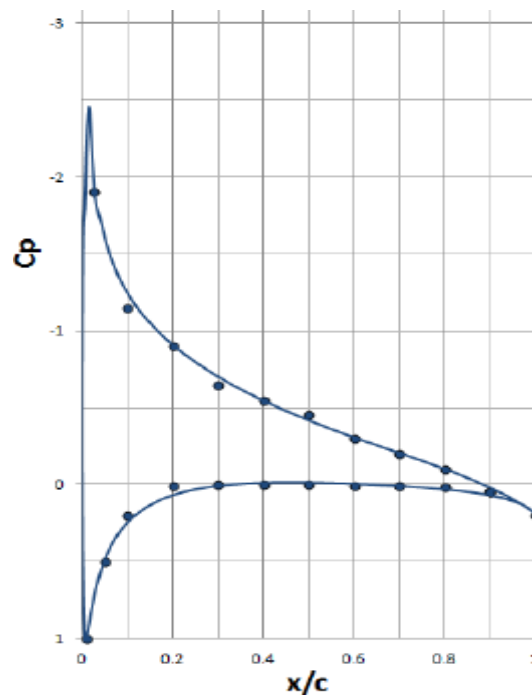


Figure (11) pressure coefficient with x axis at 1.86 angle of attack

Overall results are in good agreement with experiments in the entire range of angles of attack under analysis.

## 6 Conclusion

This case studies the flow over a NACA 0012 airfoil profile. Geometry was created using the blockMesh file. SimpleFoam solver with Spallart-Allmaras turbulent model had chosen to simulate the case. The initial condition and boundary condition are adjusted to simulate the case. Grid independent test is shown. Velocity field, and pressure field had shown with zero angle of attack. Pressure distribution over the airfoil, is evaluated. Lift coefficient as a function

of the angle of attack had been calculated. Numerical calculations of the 2-D flow over the airfoil are presented, and results are compared against the experimental results of two-dimensional wind tunnel tests of the symmetrical NACA 0012 airfoil reported in reference [1].

### References:

1. Two-dimensional aerodynamic characteristics of the NACA 0012 airfoil in the Langley 8-foot transonic pressure tunnel. NASA Technical Memorandum 81927. 1981.  
([https://www.compassis.com/downloads/Manuals/Validation/old\\_validation\\_manuals](https://www.compassis.com/downloads/Manuals/Validation/old_validation_manuals))
2. Eleni, Douvi C., Tsavalos I. Athanasios, and Margaris P. Dionissios. "Evaluation of the turbulence models for the simulation of the flow over a National Advisory Committee for Aeronautics (NACA) 0012 airfoil." *Journal of Mechanical Engineering Research* 4.3 (2012): 100-111.